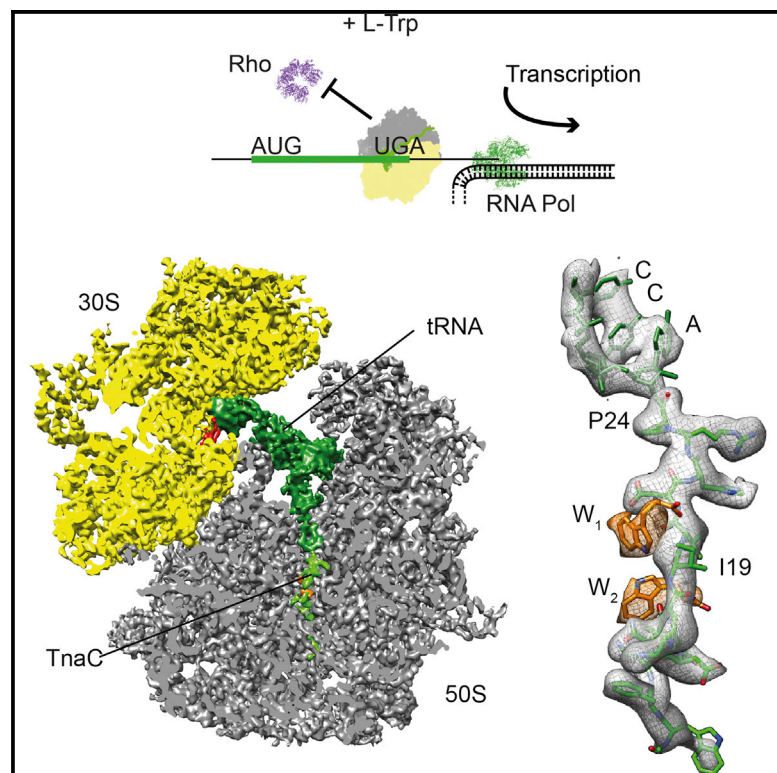


Cell Reports

Molecular Basis for the Ribosome Functioning as an L-Tryptophan Sensor

Graphical Abstract



Authors

Lukas Bischoff, Otto Berninghausen, Roland Beckmann

Correspondence

beckmann@lmb.uni-muenchen.de

In Brief

Bischoff et al. now present a cryoelectron microscopy reconstruction of a TnaC stalled ribosome, revealing two L-Trp molecules in the ribosomal exit tunnel. As a result, the peptidyl transferase center adopts a distinct conformation that precludes productive accommodation of release factor 2.

Highlights

Cryo-EM structure of a tryptophan-dependent TnaC-stalled ribosome

Molecular basis for sensing of small molecules by a ribosome nascent chain complex

Global rearrangements at the active site prevent peptide release

Accession Numbers

4UY8



Molecular Basis for the Ribosome Functioning as an L-Tryptophan Sensor

Lukas Bischoff,¹ Otto Berninghausen,¹ and Roland Beckmann^{1,*}¹Gene Center and Center for integrated Protein Science Munich, Department of Biochemistry, Feodor-Lynen-Strasse 25, University of Munich, 81377 Munich, Germany*Correspondence: beckmann@lmb.uni-muenchen.de<http://dx.doi.org/10.1016/j.celrep.2014.09.011>This is an open access article under the CC BY-NC-ND license (<http://creativecommons.org/licenses/by-nc-nd/3.0/>).

SUMMARY

Elevated levels of the free amino acid L-tryptophan (L-Trp) trigger expression of the tryptophanase *tnaCAB* operon in *E. coli*. Activation depends on tryptophan-dependent ribosomal stalling during translation of the upstream TnaC peptide. Here, we present a cryoelectron microscopy (cryo-EM) reconstruction at 3.8 Å resolution of a ribosome stalled by the TnaC peptide. Unexpectedly, we observe two L-Trp molecules in the ribosomal exit tunnel coordinated within composite hydrophobic pockets formed by the nascent TnaC peptide and the tunnel wall. As a result, the peptidyl transferase center (PTC) adopts a distinct conformation that precludes productive accommodation of release factor 2 (RF2), thereby inducing translational stalling. Collectively, our results demonstrate how the translating ribosome can act as a small molecule sensor for gene regulation.

INTRODUCTION

An increasing number of regulatory peptides are known to stall the translating ribosome during their own synthesis. Induction of stalling can be an intrinsic property of the nascent chain or can be triggered by the presence of specific small molecules (Ito and Chiba, 2013). In order to regulate gene expression, the translating ribosome can thereby be turned into a highly specific sensor for small molecules or alternatively also into a sensor for mechanical force (Ito and Chiba, 2013).

The expression of the *tna* operon in *E. coli* is controlled using a feedback loop requiring the small molecule L-tryptophan (L-Trp): the L-Trp catabolizing enzyme tryptophanase (TnaA) and the tryptophan-specific permease (TnaB) are localized downstream of the regulatory peptide TnaC. The spacer region between *tnaC* and *tnaA* contains several Rho-dependent transcription termination sites. In the absence of free L-Trp, translation of *tnaC* is efficiently terminated at the stop codon by release factor 2 (RF2), and the ribosome is dissociated (Gong and Yanofsky, 2002). This enables the transcription termination factor Rho to bind to the mRNA and terminate transcription prior to synthesis of the

tnaAB mRNA. In contrast, in the presence of inducing levels of free L-Trp peptide release by RF2 is inhibited (Gong et al., 2001). Hence, the ribosome stalls on the TnaC mRNA carrying a peptidyl-tRNA with a C-terminal proline (P24) in the P-site and a UGA stop codon in the A-site. As a consequence, Rho is blocked from binding to the mRNA and, thus, allows the transcription and subsequent translation of TnaB and TnaA (Figure 1A) (Gong and Yanofsky, 2002).

Extensive mutational studies revealed that specific amino acids of TnaC, such as P24, D16, and W12 (Cruz-Vera et al., 2005; Cruz-Vera and Yanofsky, 2008; Gong and Yanofsky, 2002) as well as their relative position to each other, are crucial for the ribosome to efficiently respond to L-Trp and induce translational stalling. In addition, numerous mutations in the ribosomal exit tunnel modulate tryptophan-dependent TnaC stalling, suggesting that the ribosome and the TnaC peptide cooperate to monitor tryptophan levels (Ito and Chiba, 2013).

A previous cryo-EM structure of a TnaC-stalled ribosome complex demonstrated that TnaC stalls the ribosome indeed with a peptidyl-tRNA remaining in the ribosomal P-site. The nascent peptide adopts a defined conformation within the ribosomal exit tunnel, and contacts between TnaC and components of the tunnel wall were identified (Seidelt et al., 2009). However, due to limited resolution it was impossible to identify how the ribosome and TnaC sense the presence of the key regulator L-Trp and how this leads to inhibition of peptidyl transferase center (PTC) activity (Seidelt et al., 2009).

RESULTS AND DISCUSSION

Cryo-EM Structure of a TnaC-Stalled Ribosome

To elucidate the molecular mechanism by which the TnaC peptide induces translational stalling in a strictly L-Trp dependent manner, we first purified TnaC-stalled ribosomes from whole *E. coli* cells (Bischoff et al., 2014) in the presence of L-Trp. Affinity purification yielded a very homogenous sample with uniformly stalled nascent chains. Cryo-EM, in combination with single-particle analysis and in silico sorting (Figure S1), resulted in a reconstruction of a ribosome population with a peptidyl-tRNA in the ribosomal P-site that was refined to an overall resolution of 3.8 Å (Figures 1B, 1C, and S2). Calculation of the local resolution (Kucukelbir et al., 2014) revealed that features in the conserved core of the ribosome were in part better resolved than the average resolution (Figure S2). Rigid-body docking of

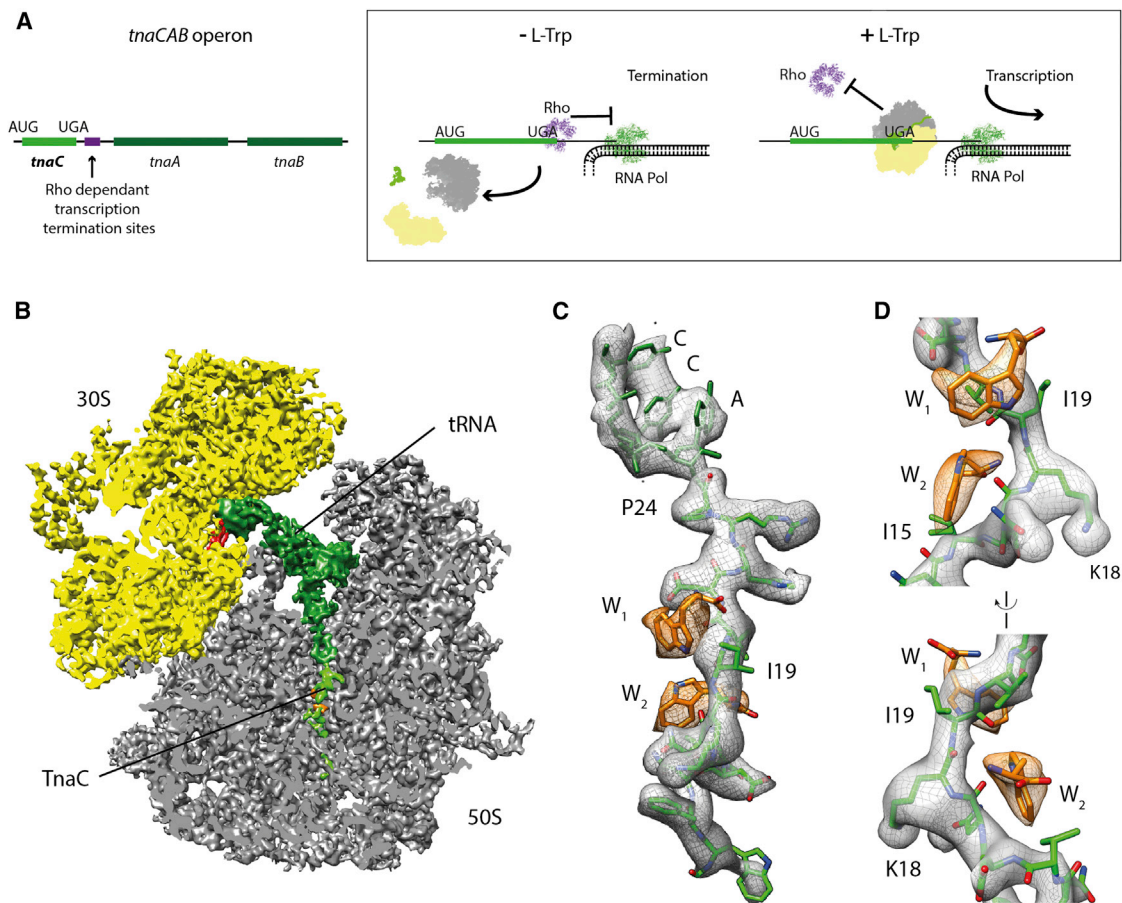


Figure 1. Cryo-EM Structure of a TnaC-Stalled Ribosome Nascent Chain Complex

(A) Schematic for the tryptophan dependent regulation of the *tna* operon in *E. coli*.

(B) Cross-section through the cryo-EM density of the TnaC-RNC, with 30S in yellow, 50S in gray, P-tRNA in dark green, and the nascent chain in light green. The mRNA anticodon is colored in red, and the free tryptophan molecules in the ribosomal exit tunnel are orange.

(C) Density and model for the TnaC nascent chain attached to the CCA end of the P-tRNA with the two additional densities of the free tryptophan molecules W_1 and W_2 .

(D) Close up on the two free tryptophan molecules interacting with hydrophobic residues of the TnaC nascent chain.

a crystallography-based molecular model of the *E. coli* large ribosomal subunit (Dunkle et al., 2010) (PDB 3OFR) revealed very good agreement of the structural details in our map with the molecular features of the model (Figure S2). As expected, the pitch of α helices, strand separation in β sheets, as well as density of large side chains were observable throughout the entire map (Figures 1C, 1D, and S2). Moreover, we found continuous and well resolved density for the nascent TnaC peptide comprising the entire C-terminal part that is critical for stalling (Cruz-Vera et al., 2005; Cruz-Vera and Yanofsky, 2008; Gong and Yanofsky, 2002). A molecular model was built de novo for this part of the TnaC peptide, and the conformation of a few rRNA bases and amino acids of the ribosomal tunnel was also adjusted (see Experimental Procedures) (Figures 1B–1D). After these adjustments, two unassigned extra densities were identified in the upper region of the exit tunnel resembling the shape of the free amino acid L-Trp (Figures 1C, 1D, and S3). Earlier biochemical studies suggested that the binding site of the free

L-Trp may be located directly in the A-site of the PTC and that it may overlap with the binding site of the antibiotic sparsomycin (Cruz-Vera et al., 2006, 2007; Cruz-Vera and Yanofsky, 2008). However, this view was recently challenged in a careful mutational analysis (Martinez et al., 2014). Indeed, our cryo-EM reconstruction cannot provide any evidence for tryptophan binding within the PTC. In contrast, we observe clear density for not only one but two free L-Trp molecules directly within the ribosomal tunnel, located 15–20 Å from the PTC.

Interactions of TnaC with Components of the Ribosomal Tunnel

The two L-Trp molecules are bound within two hydrophobic pockets formed by the TnaC nascent chain between residues D21 and N17, and rRNA nucleotides of the 23S rRNA (Figures 2A and 2B). Specifically, the first L-Trp (W_1) is bound close to V20 and I19 of TnaC and establishes stacking interactions with U2586 of the rRNA (Figure 2C). The W_1 is additionally stabilized

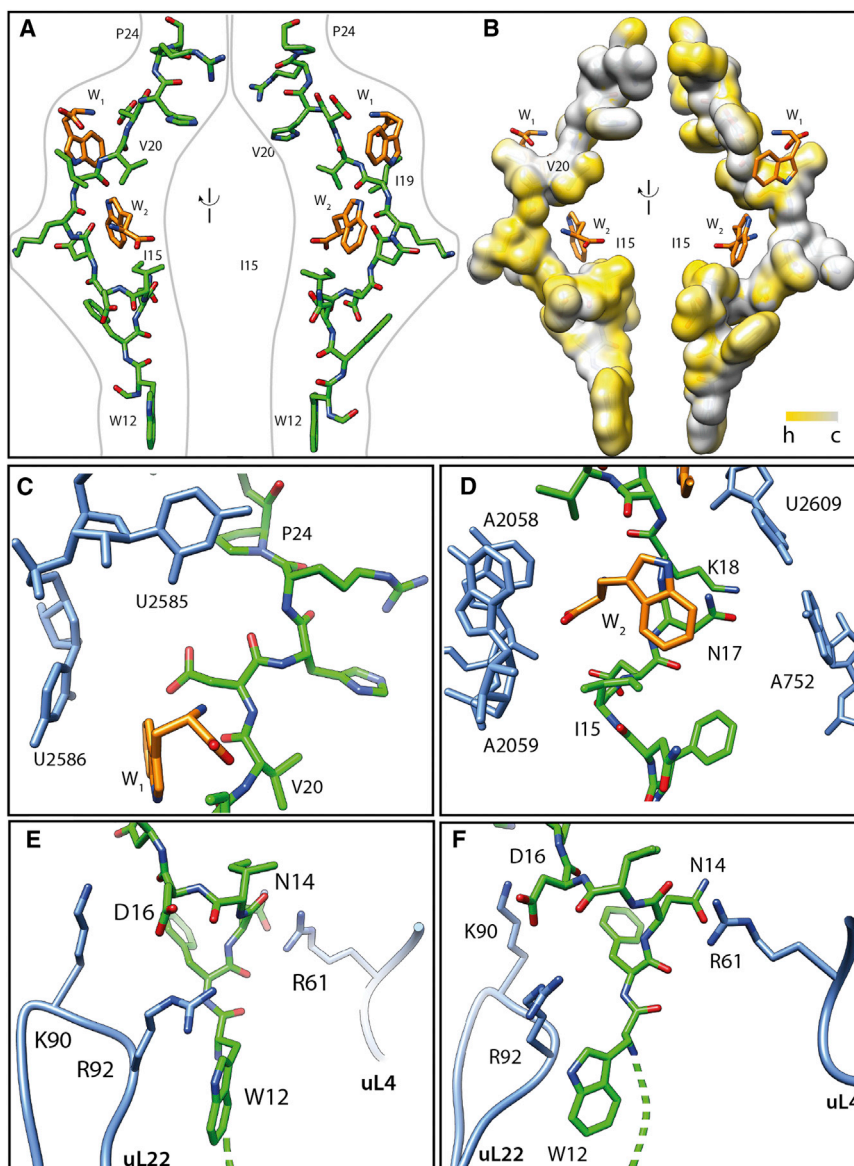


Figure 2. Interactions of TnaC with the Free L-Trp Molecules and the Ribosomal Exit Tunnel

(A) Molecular model of TnaC and the free tryptophan molecules in a schematic ribosomal exit tunnel.

(B) Surface hydrophobicity plot (h, hydrophobic; c, charged) of the nascent chain reveals two hydrophobic pockets, formed by residues V20, I19, and I15 of TnaC engaging the free tryptophan molecules.

(C) W_1 interacts with V20 and I19 of TnaC and forms a stacking interaction with U2586 of the 23S rRNA.

(D) W_2 bound in a hydrophobic pocket formed by I19 and I15 interacts with A2058 and A2059 of the 23S rRNA.

(E) The invariant residues D16 and W12 engage in a “zipper”-like interaction with K90 and R92 of the ribosomal protein uL22 of the central constriction.

(F) TnaC residue N14 interacts with R61 of uL4 on the opposite site of uL22 in the central constriction.

See also Figure S3.

Although distinct density enabled the majority of side chains in the TnaC nascent peptide to be assigned, I19 and I15 lack a clearly defined conformation. This suggests that they are not involved in direct contacts with the ribosomal exit tunnel as proposed in earlier molecular dynamics simulations but rather provide a hydrophobic environment that facilitates binding of the L-Trp molecules. Together with the TnaC nascent chain, W_2 forms a compact “bridge” or “plug” between the A2058/A2059 crevice on one side of the tunnel and the U2609/A752 base pair on the other (Figure 2D). This “bridge” resembles the ketolide telithromycin that bridges the ribosomal tunnel using a very similar geometry and by doing so induces translational arrest during translation of certain peptides (Dunkle et al., 2010) (Figure S4). These findings suggest a general role for the bases A2058, A2059, and the base pair U2609/A752 in the allosteric control of the ribosome, because this area is the target site for various small molecules ligands.

by D21 and the peptide backbone of the nascent chain. Interestingly, the nascent chain forms a sharp kink in the vicinity of N17 and K18, which is stabilized by interactions of these two amino acids with the rRNA base pair U2609 and A752 (Figure 2D). This kink results in a second hydrophobic cavity formed by V20 and I15 of the TnaC peptide (Figure 2D) that accommodates the second L-Trp (W_2). W_2 also interacts with the rRNA bases A2058 and A2059 that form a crevice in the tunnel wall that comprises the binding site of macrolide antibiotics (Dunkle et al., 2010) (Figure S4). Consistent with the composition of these binding pockets, mutation of U2609 and A752 and mutations of A2058 have been shown to severely reduce the efficiency of TnaC stalling (Cruz-Vera et al., 2005; Cruz-Vera and Yanofsky, 2008; Gong and Yanofsky, 2002). Moreover, mutation of I19 of the TnaC peptide to amino acids other than the chemically very similar leucine also affects stalling (Martínez et al., 2014).

Deeper in the ribosomal tunnel, we observe additional interactions between TnaC and the ribosomal proteins uL22 and uL4 that form the central constriction. The invariant residues D16 and W12 of the nascent chain form a “zipper”-like motif with the residues K90 and R92 of uL22 (Figures 2E, 2F, and S3). This motif may explain the particular importance of these residues for TnaC-induced stalling, for example, mutations of K90 in uL22 reduce stalling (Cruz-Vera et al., 2005, 2007), and the distance of D16 and W12 of TnaC from the PTC is also critical (Cruz-Vera et al., 2005; Cruz-Vera and Yanofsky, 2008; Gong and

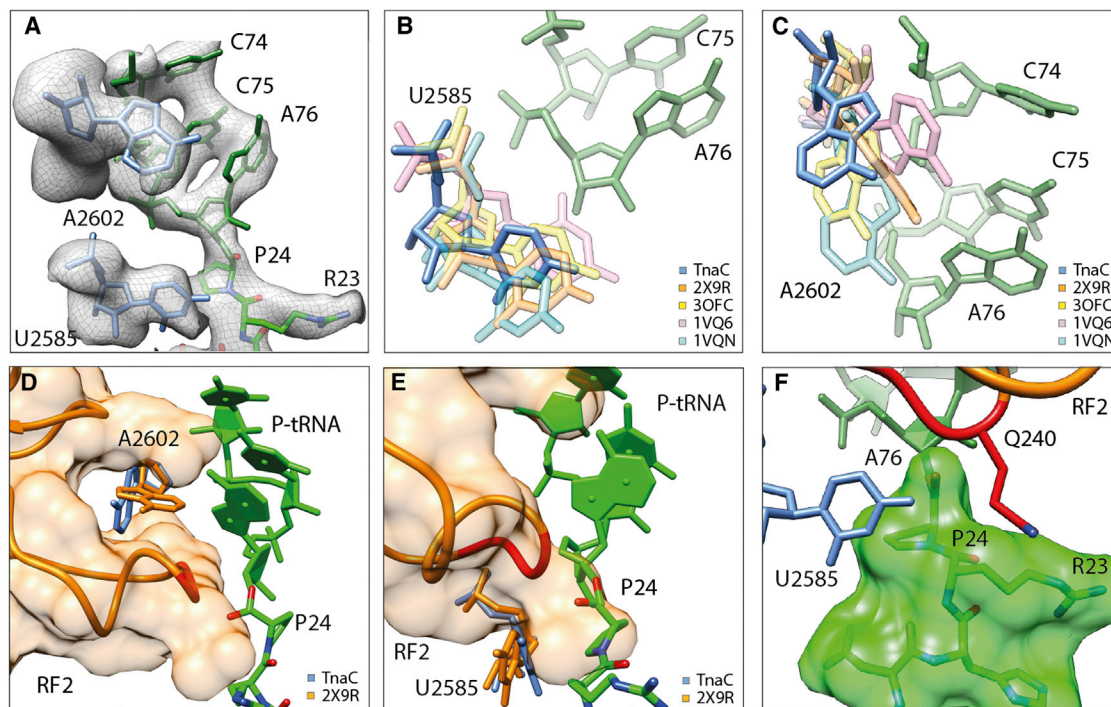


Figure 3. Silencing of the PTC in the TnaC-Stalled Ribosome

(A) The cryo-EM density for the 23S rRNA nucleotides U2585 and A2602 adopting distinct conformations in the PTC of the TnaC stalled ribosome. (B) Conformation of 23S nucleotide U2585 in TnaC (blue) in comparison to a ribosome bound to the antibiotic chloramphenicol (Dunkle et al., 2010) (PDB 3OFC, yellow), the uninduced (PDB 1VQ6, pink), and the induced (PDB 1VQN, light blue) state of the PTC (Schmeing et al., 2005a, 2005b). (C) Conformation of 23S rRNA nucleotide A2602 in TnaC (blue) in comparison to a ribosome bound to the antibiotic chloramphenicol (Dunkle et al., 2010) (PDB 3OFC, orange), the uninduced (PDB 1VQ6, pink), and the induced (PDB 1VQN, light blue) state of the PTC (Schmeing et al., 2005a, 2005b). (D) The conformation of A2602 in TnaC-SRC is inconsistent with the accommodation of release factor 2 (space filled model, orange, GGQ motive colored in red). The rotation of TnaC A2602 in comparison to A2602 in the 70S-RF2 complex (Jin et al., 2010) (PDB 2X9R, orange) leads to a clash of the nucleotide with RF2. (E) U2585 in the conformation observed in TnaC-RNC would clash with RF2 (orange space filled, GGQ motive colored in red). (F) The contact of U2585 to P24 of TnaC leads to a stabilization of R23 of TnaC (green space filled) in a position that would clash with the correct accommodation of the GGQ motive of RF2.

See also Figure S4

Yanofsky, 2002). These interactions were indeed proposed to be of significance in a molecular dynamics simulation (Trabuco et al., 2010). An additional stabilization of the “zipper” motif is established by an interaction of TnaC and ribosomal protein uL4, specifically between N14 of TnaC and R61 of uL4 (Figures 2E and 2F), the importance of which is also supported by mutational analysis of N14 (Gish and Yanofsky, 1995).

Inactivation of the Peptidyl Transferase Center

The question remains as to how these interactions within the tunnel can lead to silencing of the PTC in a manner that allows RF2 binding to the ribosome but prevents RF2-mediated release of the TnaC peptide (Gong et al., 2001; Gong and Yanofsky, 2001). Peptide-bond formation and peptide release strictly require precise positioning of the substrates, the peptidyl-tRNA and either A-tRNA or the GGQ motif of the release factor, respectively. In addition, highly conserved rRNA residues in the PTC such as U2585 and A2602 are required to dynamically adopt specific conformations depending on the functional state of the ribosome (Schmeing et al., 2005a, 2005b, 2002, 2009). Notably, the PTC of the TnaC stalled ribosomes adopts a

defined state with stabilized conformations of U2585 and A2602 (Figures 3A–3C). These conformations appear in both cases to be incompatible with productive RF2 accommodation. When comparing our structure with the crystal structure of an RF2-bound ribosome (Jin et al., 2010), it is apparent that U2585 as well as A2602 would clash with the GGQ motif of RF2 (Figures 3D and 3E). In contrast to RF2, accommodated aminoacyl-tRNA in the A-site would not clash with the observed conformation of U2585 and A2602, thus explaining why replacing the stop codon in the TnaC peptide with a canonical (non-rare) sense codon alleviates stalling (Cruz-Vera et al., 2006, 2009; Martínez et al., 2014). However, placing the rare isoleucine codon AUA in place of the stop codon induces stalling on the TnaC leader peptide (Cruz-Vera et al., 2006). This is in agreement with the idea of a general mechanism of kinetic competition between L-Trp binding in the tunnel and A-site ligand accommodation that would apply to both, release factors and aa-tRNAs. A role for such a kinetic component would also be consistent with the slow puromycin reactivity being inhibited by TnaC and with the requirement of the kinetically slower proline as ultimate amino acid.

microfluidizer (M-110L, Microfluidics) and debris was removed by centrifugation for 20 min at 16,000 rpm in a SS34 rotor (Sorvall). The cleared lysate was centrifuged through a sucrose cushion (750 mM sucrose) in buffer A at 25,000 rpm for 20 hr in a Ti45 rotor (Beckman Coulter). The crude ribosomal pellet was resuspended in a small volume of buffer A.

Ribosomes carrying the nascent chain were separated by affinity chromatography using Talon beads (Clontech Laboratories), that were additionally preincubated with 10 $\mu\text{g}/\text{ml}$ *E. coli* tRNAs to minimize unspecific binding of ribosomes. After incubating for 1 hr at 4°C, the beads were washed with at least ten column volumes (CVs) of buffer B (50 mM HEPES [pH 7.2], 500 mM KOAc, 25 mM MgCl_2 , 0.1% DDM, 2 mM tryptophan). RNCs were eluted in buffer B + 150 mM imidazole and loaded on a linear sucrose gradient 10%–40% sucrose in buffer B. After spinning for 3 hr at 40,000 rpm in a SW40 rotor (Beckman Coulter), the 70S peak was collected and diluted three times with buffer B. RNCs were finally concentrated by spinning for 4 hr at 40,000 rpm in a Ti70 rotor (Beckman Coulter) and resuspended in an appropriate volume of grid buffer (20 mM HEPES [pH 7.2], 50 mM KOAc, 5 mM $\text{Mg}[\text{OAc}]_2$, 125 mM sucrose, 2 mM tryptophan, 0.03% DDM).

Cryo-EM Specimen Preparation and Data Collection

Freshly prepared FtsQ85-TnaC RNCs (4 A_{260}/ml) was mixed with a five times excess of *E. coli* signal recognition particle and applied to 2 nm precoated Quantifoil R3/3 holey carbon supported grids and vitrified using a Vitrobot Mark IV (FEI Company). Cryo-EM data were collected at NeCEN (Leiden) on a Titan Krios TEM (FEI Company) operated at 300 keV equipped with a Cs-corrector and a back-thinned FEI Falcon II direct electron detector. The camera was calibrated for a nominal magnification of 125,085 \times resulting and a pixel size of 1.10 Å at the specimen. Frames (8 s^{-1}) were recorded in automatic mode with a dose of 4 $\text{e}^-/\text{Å}^2$ per frame at defocus values between 0.8 and 2.2 μm . The first and the last image were excluded from the data set. The remaining frames were aligned using the Gatan Microscopy suite 2.30.463.1 and subsequently summed up using the SPIDER (Frank et al., 1996) command AD S.

Cryo-EM Data Processing

The images were manually inspected, and micrographs showing drift or contamination were discarded from the data set. Subsequently, the particles were picked automatically using the software SIGNATURE (Chen and Grigorieff, 2007).

The data set of 254,000 particles was processed using the SPIDER (Frank et al., 1996) software package. It was first cleaned from nonribosomal particles (217,861 ribosomal particles left) and then sorted for the presence of a stoichiometric, homogenous P-site tRNA. The 145,393 particles that were sorted out in this step showed A/P hybrid tRNA, E site tRNA, SRP bound close to the ribosomal exit tunnel, as well as undefined density in the A-site and were not included in further refinement (Figure S1). A final subdata set of 72,468 particles with homogenous, stoichiometric density for P-site tRNA was refined to a final average resolution of 3.8 Å. To exclude potential overfitting, the data were processed using a frequency limited refinement protocol by truncating high frequencies (low-pass filter at 8 Å) during the whole refinement process (Scheres and Chen, 2012). In order to redundantly confirm for the obtained structure the lack of any potential overfitting and for validating the molecular model, the data set was also refined applying the “gold-standard” procedure. To this end, the data set was split in two halves, and each half was refined independently. As expected, the resolution judged by gold-standard Fourier shell correlation (FSC 0.143) is identical to the one obtained by the frequency limited refinement protocol (Figure S2). The final volume was B-factor sharpened using the program EM-BFACTOR (Fernández et al., 2008). The local resolution was determined using the software ResMap.

Model Building

For the interpretation of the obtained cryo-EM density, we fitted the structure of an *E. coli* 70S ribosome that was cocrystallized with the antibiotic erythromycin as a rigid body (Dunkle et al., 2010) (PDB 3OFR) using UCSF Chimera (Pettersen et al., 2004). The experimental density showed excellent agreement with the fitted crystal structure. The model for the P-site tRNA was fitted by rigid-body docking of a previous model (Seidelt et al., 2009) (PDB 2WWL,

2WWQ); the model for amino acids 12–24 of the TnaC leader peptide was both built de novo and refined using COOT (Emsley and Cowtan, 2004). The surface of the ribosomal exit tunnel until the central constriction and the PTC was carefully inspected and six bases (U2585, U2586, A2602, U2609, G2608, A752) and three side chains of amino acids of the proteins uL22 (K90 and R92) and uL4 (R61) of the central constriction were adjusted and refined using COOT (Emsley and Cowtan, 2004) to fit the experimental density (see also Figure S3). After building of the model for the nascent chain and the tunnel wall, two additional small and isolated densities remained unexplained in the ribosomal tunnel that based on their size and flat shape were interpreted representing two free L-tryptophane molecules.

To test for overfitting, the model was used to calculate FSCs with both (gold standard) half volumes. Both curves nearly overlap, indicating that the model has not been overfitted (Figure S2).

Figure Preparation

All figures showing molecular models and electron densities were prepared with the software UCSF Chimera (Pettersen et al., 2004).

ACCESSION NUMBERS

The cryo-EM map and associated atomic coordinates have been deposited in the EMDB and PDB with the accession codes EMDB-2773 and PDB ID 4UY8, respectively.

SUPPLEMENTAL INFORMATION

Supplemental Information includes four figures and one table and can be found with this article online at <http://dx.doi.org/10.1016/j.celrep.2014.09.011>.

AUTHOR CONTRIBUTIONS

L.B. and R.B. conceived the study. L.B. performed RNC purification, processed the cryo-EM data, and built molecular models. O.B. did cryo-EM screening and helped with data collection. L.B. and R.B. analyzed data and wrote the manuscript.

ACKNOWLEDGMENTS

We would like to thank C. Ungewickell for assistance with cryo-EM in Munich and Rishi Matadeen and Sacha DeCarlo for data collection at the NeCEN facility (Leiden, Netherlands). L.B. was supported by the International Max Planck Research School (IMPRS-ls); R.B. is supported by the Deutsche Forschungsgemeinschaft (DFG) through grants SFB646, GRK1721, QBM, and the Center for Integrated Protein Science and the European Research Council (Advanced Grant CRYOTRANSLATION).

Received: July 14, 2014

Revised: August 22, 2014

Accepted: September 5, 2014

Published: October 9, 2014

REFERENCES

- Bischoff, L., Wickles, S., Berninghausen, O., van der Sluis, E.O., and Beckmann, R. (2014). Visualization of a polytopic membrane protein during SecY-mediated membrane insertion. *Nat. Commun.* 5, 4103.
- Chen, J.Z., and Grigorieff, N. (2007). SIGNATURE: a single-particle selection system for molecular electron microscopy. *J. Struct. Biol.* 157, 168–173.
- Cruz-Vera, L.R., and Yanofsky, C. (2008). Conserved residues Asp16 and Pro24 of TnaC-tRNA^{Pro} participate in tryptophan induction of Tna operon expression. *J. Bacteriol.* 190, 4791–4797.
- Cruz-Vera, L.R., Rajagopal, S., Squires, C., and Yanofsky, C. (2005). Features of ribosome-peptidyl-tRNA interactions essential for tryptophan induction of tna operon expression. *Mol. Cell* 19, 333–343.

- Cruz-Vera, L.R., Gong, M., and Yanofsky, C. (2006). Changes produced by bound tryptophan in the ribosome peptidyl transferase center in response to TnaC, a nascent leader peptide. *Proc. Natl. Acad. Sci. USA* *103*, 3598–3603.
- Cruz-Vera, L.R., New, A., Squires, C., and Yanofsky, C. (2007). Ribosomal features essential for tna operon induction: tryptophan binding at the peptidyl transferase center. *J. Bacteriol.* *189*, 3140–3146.
- Cruz-Vera, L.R., Yang, R., and Yanofsky, C. (2009). Tryptophan inhibits *Proteus vulgaris* TnaC leader peptide elongation, activating tna operon expression. *J. Bacteriol.* *191*, 7001–7006.
- Dunkle, J.A., Xiong, L., Mankin, A.S., and Cate, J.H. (2010). Structures of the *Escherichia coli* ribosome with antibiotics bound near the peptidyl transferase center explain spectra of drug action. *Proc. Natl. Acad. Sci. USA* *107*, 17152–17157.
- Emsley, P., and Cowtan, K. (2004). Coot: model-building tools for molecular graphics. *Acta Crystallogr. D Biol. Crystallogr.* *60*, 2126–2132.
- Fernández, J.J., Luque, D., Castón, J.R., and Carrascosa, J.L. (2008). Sharpening high resolution information in single particle electron cryomicroscopy. *J. Struct. Biol.* *164*, 170–175.
- Frank, J., Radermacher, M., Penczek, P., Zhu, J., Li, Y., Ladjadj, M., and Leith, A. (1996). SPIDER and WEB: processing and visualization of images in 3D electron microscopy and related fields. *J. Struct. Biol.* *116*, 190–199.
- Gish, K., and Yanofsky, C. (1995). Evidence suggesting cis action by the TnaC leader peptide in regulating transcription attenuation in the tryptophanase operon of *Escherichia coli*. *J. Bacteriol.* *177*, 7245–7254.
- Gong, F., and Yanofsky, C. (2001). Reproducing tna operon regulation in vitro in an S-30 system. Tryptophan induction inhibits cleavage of TnaC peptidyl-tRNA. *J. Biol. Chem.* *276*, 1974–1983.
- Gong, F., and Yanofsky, C. (2002). Instruction of translating ribosome by nascent peptide. *Science* *297*, 1864–1867.
- Gong, F., Ito, K., Nakamura, Y., and Yanofsky, C. (2001). The mechanism of tryptophan induction of tryptophanase operon expression: tryptophan inhibits release factor-mediated cleavage of TnaC-peptidyl-tRNA(Pro). *Proc. Natl. Acad. Sci. USA* *98*, 8997–9001.
- Hansen, J.L., Moore, P.B., and Steitz, T.A. (2003). Structures of five antibiotics bound at the peptidyl transferase center of the large ribosomal subunit. *J. Mol. Biol.* *330*, 1061–1075.
- Ito, K., and Chiba, S. (2013). Arrest peptides: cis-acting modulators of translation. *Annu. Rev. Biochem.* *82*, 171–202.
- Jin, H., Kelley, A.C., Loakes, D., and Ramakrishnan, V. (2010). Structure of the 70S ribosome bound to release factor 2 and a substrate analog provides insights into catalysis of peptide release. *Proc. Natl. Acad. Sci. USA* *107*, 8593–8598.
- Kucukelbir, A., Sigworth, F.J., and Tagare, H.D. (2014). Quantifying the local resolution of cryo-EM density maps. *Nat. Methods* *11*, 63–65.
- Martinez, A.K., Gordon, E., Sengupta, A., Shirole, N., Klepacki, D., Martinez-Garriga, B., Brown, L.M., Benedik, M.J., Yanofsky, C., Mankin, A.S., et al. (2014). Interactions of the TnaC nascent peptide with rRNA in the exit tunnel enable the ribosome to respond to free tryptophan. *Nucleic Acids Res.* *42*, 1245–1256.
- Pavlov, M.Y., Watts, R.E., Tan, Z., Cornish, V.W., Ehrenberg, M., and Forster, A.C. (2009). Slow peptide bond formation by proline and other N-alkylamino acids in translation. *Proc. Natl. Acad. Sci. USA* *106*, 50–54.
- Pettersen, E.F., Goddard, T.D., Huang, C.C., Couch, G.S., Greenblatt, D.M., Meng, E.C., and Ferrin, T.E. (2004). UCSF Chimera—a visualization system for exploratory research and analysis. *J. Comput. Chem.* *25*, 1605–1612.
- Scheres, S.H., and Chen, S. (2012). Prevention of overfitting in cryo-EM structure determination. *Nat. Methods* *9*, 853–854.
- Schmeing, T.M., Seila, A.C., Hansen, J.L., Freeborn, B., Soukup, J.K., Scaringe, S.A., Strobel, S.A., Moore, P.B., and Steitz, T.A. (2002). A pre-translocational intermediate in protein synthesis observed in crystals of enzymatically active 50S subunits. *Nat. Struct. Biol.* *9*, 225–230.
- Schmeing, T.M., Huang, K.S., Kitchen, D.E., Strobel, S.A., and Steitz, T.A. (2005a). Structural insights into the roles of water and the 2' hydroxyl of the P site tRNA in the peptidyl transferase reaction. *Mol. Cell* *20*, 437–448.
- Schmeing, T.M., Huang, K.S., Strobel, S.A., and Steitz, T.A. (2005b). An induced-fit mechanism to promote peptide bond formation and exclude hydrolysis of peptidyl-tRNA. *Nature* *438*, 520–524.
- Schmeing, T.M., Voorhees, R.M., Kelley, A.C., Gao, Y.G., Murphy, F.V., 4th, Weir, J.R., and Ramakrishnan, V. (2009). The crystal structure of the ribosome bound to EF-Tu and aminoacyl-tRNA. *Science* *326*, 688–694.
- Seidelt, B., Innis, C.A., Wilson, D.N., Gartmann, M., Armache, J.P., Villa, E., Trabuco, L.G., Becker, T., Mielke, T., Schulten, K., et al. (2009). Structural insight into nascent polypeptide chain-mediated translational stalling. *Science* *326*, 1412–1415.
- Trabuco, L.G., Harrison, C.B., Schreiner, E., and Schulten, K. (2010). Recognition of the regulatory nascent chain TnaC by the ribosome. *Structure* *18*, 627–637.